ELSEVIER

Polymer 40 (1999) 7137–7146

polymer

Synthesis and non-isothermal crystallization behaviors of poly(ethylene isophthalate-*co*-terephthalate)s

S.W. Lee[a], M. Ree[a,*], C.E. Park[b], Y.K. Jung[c], C.-S. Park[c], Y.S. Jin[c], D.C. Bae[c]

[a]*Department of Chemistry, Polymer Research Institute, School of Environmental Engineering, Pohang University of Science and Technology, San 31, Hyoja-dong, Pohang 790-784, South Korea*

[b]*Department of Chemical Engineering, Pohang University of Science and Technology, San 31, Hyoja-dong, Pohang 790-784, South Korea*

[c]*POSCO Technical Research Laboratories, Pohang Irons and Steel Company, 1 Koedong-dong, Pohang 790-785, South Korea*

Received 21 September 1998; received in revised form 22 December 1998; accepted 5 February 1999

Abstract

A series of random copolyesters with reasonably high molecular weights were synthesized with varying composition by the bulk copolycondensation of ethylene glycol with dimethyl isophthalate (DMI) and dimethyl terephthalate. Compositions and molecular weights of the copolyesters were determined by ^{1}H NMR spectroscopy and viscometry, respectively. The copolyesters containing DMI of ≤20 mol% and ≥90 mol% are crystallizable, whereas the copolyesters with DMI ≥20 mol% and ≤90 mol% are amorphous. For the copolyesters containing DMI of ≤10 mol%, crystallization behaviors were non-isothermally investigated by calorimetry and analyzed by both modified Avrami and Ozawa approaches. Regardless of the composition, the value of the Avrami exponent is 2.8–3.5, depending on the cooling rate, whereas the value of the Ozawa exponent is 2.1–2.6, depending on the temperature. These results indicate that the nucleation and growth mechanisms of the copolyesters are apparently identical to those of poly(ethylene terephthalate). However, the crystallization rate is decreased by incorporating the DMI unit into the polymer backbone and also by lowering the cooling rate. In addition, the crystallization activation energy is found to be increased by incorporating the DMI unit into the polymer backbone. However, both of the analytical approaches show a big discrepancy in the estimation of the exponent which is critical to identify the type of nucleation and growth mechanism in the non-isothermal crystallization even though they have been derived from the same Avrami approach.

Keywords: Aromatic copolyesters; Non-isothermal crystallization; Nucleation

1. Introduction

Poly(ethylene terephthalate) (PET) is widely used as synthetic fibers, packaging films, recording and photographic tapes, bottles for beverage and food, and engineering plastic components, because of the excellent thermal and mechanical properties, high chemical resistance, and low gas permeability [1–3]. However, PET polymer still has some undesirable properties: for example, poor dyeability, pilling, low moisture regain, generation of static charges, poor adhesion to metals, and poor processability due to the high melting temperature.

In general, copolymerization affords a facile means of modifying the crystallinity, morphology, melting point (T_m), glass transition temperature (T_g), solubility, permeability, etc. However, as a corollary, the use of copolymerization to modify a particular property may also alter other properties, not always desirably. For many advantages of copolymerization, there is still a great motivation for incorporating a third component into the PET polymer to overcome the undesirable properties.

Poly(ethylene isophthalate-*co*-terephthalate) (PEIT) exemplifies copolyesters possessing a crystallizing and a poorly or non-crystallizing component [3]. According to previous studies [4,5], random PEIT copolyester is known to be formed by the conventional bulk polycondensation of ethylene glycol (EG) with dimethyl isophthalate (DMI) (or isophthalic acid) and dimethyl terephthalate (DMT) (or terephthalic acid). The incorporation of DMI changes the morphology (i.e. crystallinity and crystal size) and properties (i.e. T_m, T_g, thermal expansivity, and mechanical properties) of PET homopolymer, possibly improving the low temperature processability and the adhesion to substrates such as metal and ceramic sheets. The PEIT copolyesters

* Corresponding author. Tel.: + 82-562-279-2120; fax: + 82-562-279-3399.

E-mail address: ree@postech.ac.kr (M. Ree)

0032-3861/99/$ - see front matter
PII: S0032-3861(99)00119-6

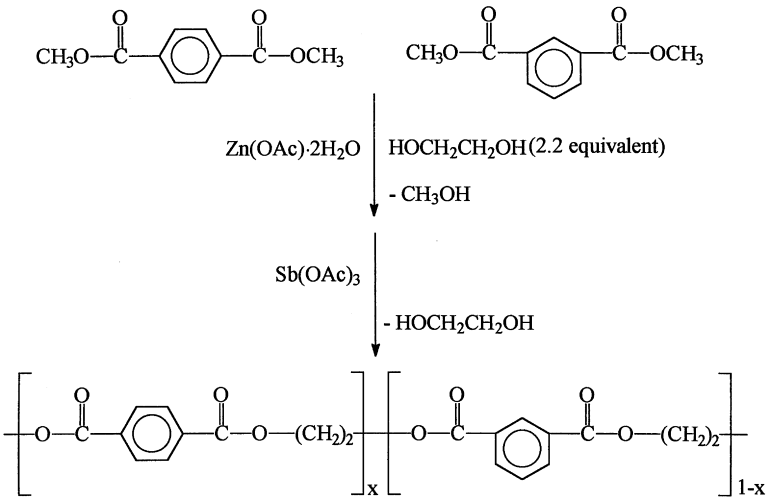

Fig. 1. Synthetic scheme of PEIT copolyesters.

are currently used in industry as thermally shrinkable package films as well as heat-sealable laminating films for steel cans and metal and ceramic sheets [5–9]. However, despite the well recognized industrial importance, PEIT copolyester did not attract the same attention, and few studies dealing with its crystallization from the molten state have appeared up to now.

In fact, properties of a crystallizable polymer are strongly dependent on the morphological structure (size, shape, perfection, volume fraction, and orientation of crystallites) which is formed by crystallization from the molten state. Thus, for crystallizable polymers, crystallization behavior is an interesting research subject to control morphological structure and to understand resultant properties. In particular, the behavior of crystallizable polymers during non-isothermal crystallization from the melt, is of increasing technological importance, because these conditions are the closest to real industrial processing conditions. Therefore, it is highly desired to investigate non-isothermal crystallization behavior for optimizing their processes and understanding properties of the processed products.

In this study, a series of PET copolyesters were synthesized with varying composition by the conventional bulk polycondensation of DMT and EG using DMI as a third component. For the copolyesters synthesized, molecular weight and composition were determined. And their non-isothermal crystallization behaviors were measured by differential scanning calorimetry and analyzed by both modified Avrami and Ozawa approaches in regard with the effect of the third component.

2. Experimental

2.1. Materials

Dimethyl isophthalate (DMI) and dimethy terephthalate (DMT) were obtained from SKC Limited, Korea. Ethylene glycol (EG) and antimony acetate were supplied from LG Chemical Company, Korea. Zinc acetate dihydrate and trimethyl phosphate were purchased from Aldrich Chemical Company, USA. All the chemicals were used as received without further purification.

2.2. Synthesis

A poly(ethylene isophthalate-*co*-terephthalate) (PEIT) of 50/50 (molar ratio) composition (DMI50) was synthesized by a two-step reaction sequence as follows (see Fig. 1). In the first step, DMT of 0.5 equivalent and DMI of 0.5 equivalent were added into EG of 2.2 equivalent in a two-neck flask equipped with a mechanically sealed stirrer and a motor, followed by adding zinc acetate dihydrate (2.7×10^{-4} wt.% of the total amount of DMI and DMT mixture) as an ester interchange reaction catalyst. After the addition was complete, a condenser was equipped into the flask. Then, the ester interchange reaction was conducted with stirring for 2.0–2.5 h at 180–210°C. During the reaction, methanol, as the by-product, was removed with a yield of 92% from the reaction mixture.

In the second step, antimony acetate (9.9×10^{-4} wt.% of the total amount of DMI and DMT mixture) and trimethyl phosphate (1.5×10^{-3} wt.% of the total amount of DMI and DMT mixture) were added into the reaction mixture as a polycondensation catalyst and a thermal stabilizer, respectively. The polymerization was carried out with stirring for 2.5–3.5 h at 260–280°C under a vacuum of ca. 1×10^{-2} Torr as described elsewhere [10].

In the same manner, a series of PEIT copolyetsers with other compositions were prepared with varying the compositions of DMI and DMT monomers.

2.3. Characterization

Compositions of the copolyesters synthesized were

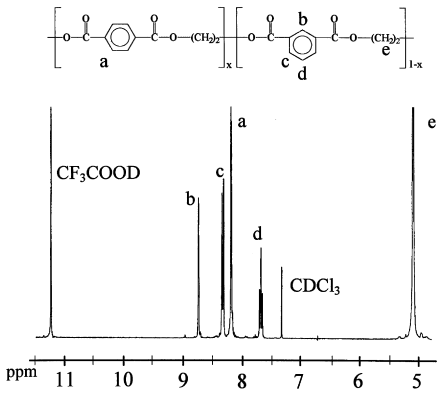

Fig. 2. ^{1}H NMR spectrum of DMI50 copolyester dissolved in a mixture (3:1 in volume) of CF_3COOD and $CDCl_3$.

determined in a $CF_3COOD/CDCl_3$ mixture (3:1 in volume) [11] using a proton nuclear magnetic resonance (^{1}H NMR) spectrometer (Bruker ASPECT 300 MHz). Intrinsic viscosity was measured in CF_3COOH at 30 ± 0.1°C using an Ubbelohde suspended level capillary viscometer [12].

Thermal characterization was performed under a dry nitrogen atmosphere using a differential scanning calorimeter (DSC) (Seiko DSC 220CU). Both temperature and heat flow were calibrated using indium and tin standards. Sample specimens of 3.0–5.0 mg were used. In the DSC measurement, a polymer sample was preheated at 290°C for 10 min in order to remove its thermal history and then cooled down to 0°C with a rate of 10.0 K/min. Subsequently, the cooled sample was again heated up to 300°C with a rate of 5.0 K/min. T_m was chosen as the temperature at the peak maximum of melting transition measured in the heating run and the heat of fusion (ΔH_f) was additionally estimated. T_g was chosen as the temperature at the middle point of glass transition obtained in the heating run.

For copolyesters containing DMI of ≤ 10 mol% which are highly crystallizable, non-isothermal crystallization was performed with varying cooling rate over 2.0–20.0 K/min. Each sample was heated up to 290°C with a rate of 80 K/min and then held at that temperature for 10 min to remove thermal history, followed by cooling to 0°C with a chosen cooling rate. Crystallization peak temperature (T_p) was estimated from the peak maximum of the DSC thermogram. In addition, the heat of crystallization (ΔH_c) was obtained from the DSC thermogram.

Table 1
Compositions, intrinsic viscosities[η], and weight average molecular weights ($\bar{M}_w$) of PEIT copolyesters

Sample designation	Feed ratio[a] (DMI/DMT)	Polyester composition[b] (DMI/DMT)	[η] (dl/g)	$\bar{M}_w$[c]
PET	0/100	0/100	0.545	36 000
DMI5	5/95	4.9/95.1	0.551	37 000
DMI10	10/90	9.8/10.2	0.542	36 000
DMI15	15/85	14.9/85.1	0.522	34 000
DMI20	20/80	19.6/80.4	0.503	32 000
DMI25	25/75	25.3/74.7	0.536	35 000
DMI30	30/70	30.2/69.8	0.547	36 000
DMI40	40/60	39.9/40.1	0.524	34 000
DMI50	50/50	50.4/49.6	0.504	32 000
DMI60	60/40	60.2/39.8	0.542	36 000
DMI70	70/30	70.7/29.3	0.451	27 000
DMI80	80/20	79.8/20.2	0.389	22 000
DMI90	90/10	90.4/9.6	0.380	21 000
PEI	100/0	100/0	0.372	21 000

[a] Molar ratio of DMI and DMT monomers fed in the polymerization.
[b] Measured by ^{1}H NMR spectroscopy.

3. Results and discussion

3.1. Synthesis

For a series of PEIT copolyesters synthesized, chemical compositions were determined by ^{1}H NMR spectroscopy. As shown in Fig. 2, the molar ratio of the DMT and DMI units on the polymer backbone was estimated from integrations of their specific chemical shifts. The results are summarized in Table 1. The determined compositions are in good agreement with the compositions of monomers fed in the first-step reaction (i.e. ester interchange reaction) within less than 2%. This result indicates that DMT and DMI monomers have an almost same reactivity in the ester interchange reaction with EG.

For the copolyesters synthesized, weight average molecular weights ($\bar{M}_w$s) were estimated from the measured intrinsic viscosities ([η]s) using the Mark–Hauwink–Sakurada equation with constants a and k which were determined previously by Wallach [12] for PET homopolymer:

$$[\eta] = 4.33 \times 10^{-4} \bar{M}_w^{0.68}. \quad (1)$$

The results are listed in Table 1. The estimated $\bar{M}_w$s are in the range of 21 000–37 000, depending on the compositions. In comparison, copolyesters rich with DMT unit have relatively higher molecular weights than those of copolymers rich with DMI unit. In fact, Eq. (1) was found for PET homopolymer rather than poly(ethylene isophthalate) (PEI) homopolymer and PEIT copolyesters. PEI homopolymer may have different values of the constants a and k from those of PET homopolymer. Thus, the relatively low $\bar{M}_w$s for both the PEI homopolymer and the DMI-unit-rich copolymers may be attributed in part to the constants a and k which are estimated incorrectly. Overall, all the copolyesters were however synthesized in reasonably high molecular weights.

3.2. Phase transition behavior

Fig. 3 shows DSC thermograms of PEIT copolyesters with various compositions which were measured by heating with a rate of 5.0 K/min after crystallized with a cooling rate of 10.0 K/min. The copolyesters containing DMI unit

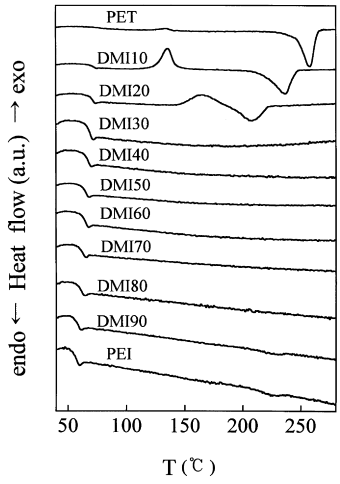

Fig. 3. DSC thermograms of PEIT copolyesters cooled with a rate of 10.0 K/min from the molten state. In the heating run, a rate of 5.0 K/min was employed.

of ≤20 mol% reveal two phase transitions: one appears over 50–80°C, which corresponds to the glass transition, and another over 180–270°C, which correspond to the melting transition of crystals. In particular, PET homopolymer shows a relatively weak glass transition. This might be due to its relatively high crystallinity. In contrast, the copolyesters with DMI unit of ≥80 mol% exhibit two transitions as observed for the copolyesters with DMI unit of ≤20 mol%. However, the melting transitions appear very weakly because of their relatively low crystallinities. This indicates that the DMI unit is a poorly crystallizable unit, which is due to the kinked *meta*-linkage. In contrast, copolyesters with 20 mol% < DMI unit < 80 mol% show

Table 2
Glass transition temperatures (T_gs), melting temperatures (T_ms), heats of fusion (ΔH_fs), and crystallinities (X_cs) of PEIT copolyesters[a]

Sample designation	T_g (°C)	T_m (°C)	ΔH_f (J/g)	X_c[b] (%)
PET	76.1	258.6	43.98	37.4
DMI5	74.6	244.8	37.80	32.1
DMI10	73.5	234.2	35.72	30.4
DMI15	72.4	220.6	29.05	24.7
DMI20	71.2	208.8	11.13	9.5
DMI25	69.9	—[c]	—	—
DMI30	68.5	—	—	—
DMI40	66.4	—	—	—
DMI50	64.1	—	—	—
DMI60	62.4	—	—	—
DMI70	60.6	—	—	—
DMI80	58.9	—	—	—
DMI90	57.2	231.0	0.80	0.7
PEI	56.0	232.4	2.39	2.0

[a] Measured by DSC with a heating rate of 5.0 K/min after crystallization with a cooling rate of 10.0 K/min from the molten state.

[b] Estimated from the measured heat of fusion against the heat of fusion (117.6 J/g) of the fully crystallized PET polymer [24].

[c] Not detected.

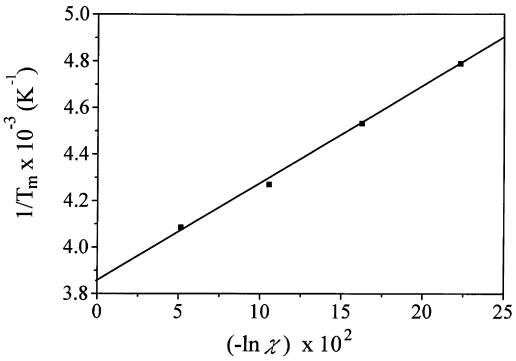

Fig. 4. Flory plot of $1/T_m$ versus $(-\ln x)$ for the PEIT copolyesters rich with DMT unit: (■), measured by DSC; (—), fitted by Eq. (2).

only one phase transition that corresponds to the glass transition, indicating that these polymers are amorphous. In addition, the PET, DMI10, and DMI20 polyesters show an exothermic peak over 120–170°C, respectively. These exotherms are due to the recrystallization occurred during the heating run.

From the DSC thermograms in Fig. 3, T_m and ΔH_f, as well as T_g were estimated. In addition, the absolute crystallinity (X_c) was calculated from the measured ΔH_c using the heat of fusion (117.6 J/g) for the completely crystallized PET [13]. The results are summarized in Table 2. For the DMT rich copolyester, T_m, ΔH_f and X_c decrease with decreasing the DMT content, respectively. Similar T_m, ΔH_f and X_c variations are observed for the DMI rich copolyester. However, ΔH_fs of the DMI rich copolyesters are relatively much smaller than those of the DMT rich copolyesters: that is, X_c is less than 2.4%.

In particular, T_ms of the DMT rich copolyesters were further analyzed by the Flory equation [14]:

$$\frac{1}{T_m} - \frac{1}{T_m^0} = -\frac{R}{\Delta H_f} \ln x \tag{2}$$

where T_m is the melting temperature of PEIT copolyester, T_m^0 the melting temperature of PET homopolymer, x the molar fraction of crystallizable DMT unit, and R the universal gas constant. As shown in Fig. 4, the plot of T_m^{-1} against $(-\ln x)$ shows a good linearity. And, the plot of T_m^{-1} is extrapolated to $x = 0$, giving $T_m^0 = 259.3$°C which is the melting temperature of PET homopolymer. This value of the T_m^0 is very close to that (258.6°C) measured for PET homopolymer.

All the PEIT copolyesters exhibit single T_gs. The T_g decreases with increasing DMI content. The T_g variation with composition was further analyzed by the Fox equation [15]:

$$\frac{1}{T_{g,co}} = \frac{w_a}{T_{g,a}} + \frac{w_b}{T_{g,b}} \tag{3}$$

where $T_{g,co}$ is the glass transition temperature of PEIT copolyester, w_a and w_b are the weight fractions of DMT and DMI comonomers, respectively, $T_{g,a}$ the glass transition

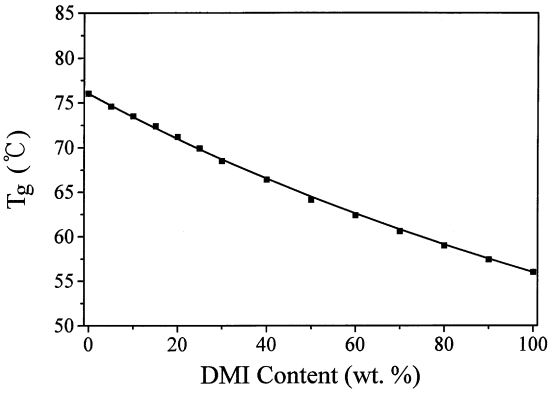

Fig. 5. Fox plot of T_g versus the DMI content for the PEIT copolyester: (■), measured by DSC; (—), fitted by Eq. (3).

temperature of PET homopolymer, and $T_{g,b}$ the glass transition temperature of PEI homopolymer. As shown in Fig. 5, the measured T_gs are fitted very well by the Fox equation.

From these results it is concluded that random PEIT copolyesters were synthesized over all the compositions. This is consistent with the result reported previously in the literature [4].

3.3. Non-isothermal crystallization behavior

For the PET homopolymer and DMI5 and DMI10 copolyesters which are crystallizable, non-isothermal crystallizations were performed from the molten state by DSC with various cooling rates over 2.0–20.0 K/min. In the DSC measurement, these polymers revealed typical crystallization exotherms as observed for common crystallizable polymers. The measured crystallization exotherms are shown in Fig. 6. For the PET homopolymer, the non-isothermal crystallization exotherm becomes broad and is shifted to the low temperature region as the cooling rate increases. Similar behaviors were observed for both DMI5 and DMI10 copolyesters.

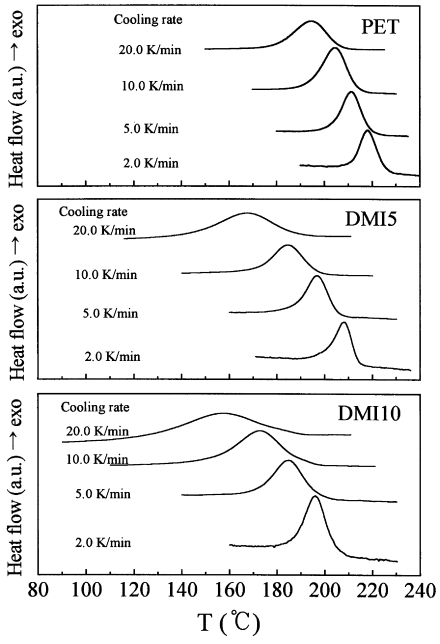

Fig. 6. Non-isothermal crystallization exotherms of PET hompolymer and PEIT copolyesters measured at various cooling rates: DMI5, PEIT (5.0 mol% DMI) copolyester; DMI10 (10.0 mol% DMI) copolyester.

In comparison, crystallization exotherm, which was measured at a chosen cooling rate, is shifted to the low temperature region as the DMI content increases. This might result mainly from the depression of crystallization temperature caused by the incorporation of poorly crystallizable DMI unit into the polymer backbone. For all the crystallization exotherms measured, peak temperature (T_p), the heat of crystallization (ΔH_c) and crystallinity (X_c) have been estimated as a function of cooling rate, and listed in Table 3. Overall, T_p, ΔH_c and X_c decrease, respectively, as the cooling rate increases. These also decrease, respectively, as the DMI content increases.

Up to date, several analytical methods have been developed in order to understand non-isothermal crystallization kinetics of polymers: (i) modified Avrami analysis [16–18], (ii) Ozawa analysis [19,20], (iii) Ziabicki analysis [21,22], and (iv) others [23–30]. In the present study, both the modified Avrami analysis and the Ozawa method have been adapted for characterizing non-isothermal crystallization processes of the PEIT copolyesters as follows.

3.3.1. Modified Avrami analysis

The Avrami equation [31–33] has been used widely to describe isothermal crystallization kinetics of polymers:

$$1 - X_t = \exp(-kt^n) \tag{4}$$

where X_t is the relative crystallinity, n is the Avrami exponent, and k is the growth rate constant. Here, the value of Avrami exponent represents the nucleation mechanism and growth dimension, and the growth rate constant is a function of the nucleation and the growth rate. The relative crystallinity X_t is defined as a function of crystallization time in the following:

$$X_t = \frac{\int_{t_0}^{t} (\mathrm{d}H_c/\mathrm{d}t)\,\mathrm{d}t}{\int_{t_0}^{t_\infty} (\mathrm{d}H_c/\mathrm{d}t)\,\mathrm{d}t} \tag{5}$$

where $\mathrm{d}H_c/\mathrm{d}t$ is the rate of heat evolution, and t_o and t_∞ represent the onset and end time of crystallization, respectively.

The Avrami analysis can be extended for non-isothermal crystallization as described previously in the literature [16–18,34]. For non-isothermal crystallization at a chosen cooling rate, the relative crystallinity X_t is a function of crystallization temperature. That is, Eq. (5) can be rewritten as follows:

$$X_t = \frac{\int_{T_0}^{T} (\mathrm{d}H_c/\mathrm{d}T)\,\mathrm{d}T}{\int_{T_0}^{T_\infty} (\mathrm{d}H_c/\mathrm{d}T)\,\mathrm{d}T} \tag{6}$$

where T is the crystallization temperature, and T_0 and T_∞

Table 3
Crystallization peak temperatures (T_ps), heats of crystallization (ΔH_cs) and crystallinities (X_cs) of PET homopolymer and PEIT copolyesters

Cooling rate (K/min)	PET homopolymer			DMI5 copolyester			DMI10 copolyester		
	T_p (°C)	ΔH_c (J/g)	X_c[a] (%)	T_p (°C)	ΔH_c (J/g)	X_c[a] (%)	T_p (°C)	ΔH_c (J/g)	X_c[a] (%)
2.0	218.1	−41.73	35.5	209.1	−41.54	35.3	198.0	−38.62	32.8
5.0	211.4	−39.92	33.9	196.7	−39.61	33.7	184.8	−35.86	30.5
10.0	204.6	−37.52	31.9	184.5	−37.36	31.8	172.6	−26.76	22.8
20.0	198.4	−35.54	30.2	171.7	−29.81	25.3	161.7	−12.28	10.4

represent the onset and end temperature of crystallization, respectively.

For example, the non-isothermal exotherms of the PET homopolymer in Fig. 6 were analyzed using Eqs. (4) and (6). The results are illustrated in Fig. 7. For each cooling run, X_t increases exponentially with decreasing temperature and finally levels off. The plot of X_t versus T is shifted to the low temperature region as the cooling rate increases.

The crystallization temperatures T and T_0 in Eq. (6) can be converted to the crystallization times t and t_0, respectively. The relationship between t and T can be expressed as [21,34]:

$$t = \frac{T_0 - T}{C} \tag{7}$$

where C is the cooling rate employed for non-isothermal crystallization. Using Eq. (7), the X_t variations with T in Fig. 7 were re-plotted in Fig. 8 as a function of crystallization time t. The plots of X_t versus t are in sigmoidal shape, suggesting that the extended Avrami analysis might be applicable for non-isothermal crystallizations of the PET homopolymer.

In order to estimate the Avrami parameters (i.e. exponent n and rate constant k), the X_t variations with t in Fig. 8 can be plotted again using Eq. (4) in a double-logarithmic form as:

$$\log[-ln(1 - X_t)] = 1\log k + n\log t. \tag{8}$$

Here, the rate of non-isothermal crystallization depends upon the cooling rate employed. Thus, the crystallization rate constant k should be corrected adequately. Assuming constant cooling rate, the final form of crystallization rate constant can be corrected as follows [34]:

$$\log k' = \frac{\log k}{C}. \tag{9}$$

Further, the crystallization half-time $t_{1/2}$, which is defined as the time at which the development of crystallization is complete by 50%, can be determined from the corrected crystallization rate constant k' as follows:

$$t_{1/2} = \left(\frac{\ln 2}{k'}\right)^{1/n}. \tag{10}$$

Fig. 9 shows the plots of $\log[-\ln(1 - X_t)]$ versus $\log t$ for non-isothermal crystallizations of the PET homopolymer. For the non-isothermal crystallization with a cooling rate of 2.0 K/min, the plot of $\log[-\ln(1 - X_t)]$ versus $\log t$ varies linearly with a slope at the early stage and then continues a linear variation with a different slope at the later stage, consequently showing a two-regime behavior. Similar two-regime behaviors are observed in the plot of $\log[-\ln(1 - X_t)]$ against $\log t$ for rapid cooling rates of 5.0–20.0 K/min. Overall, the slope in the first regime is relatively greater than that of the second regime, regardless of cooling rates.

The second regime behaviors observed might be due to the secondary crystallization. That is caused by the

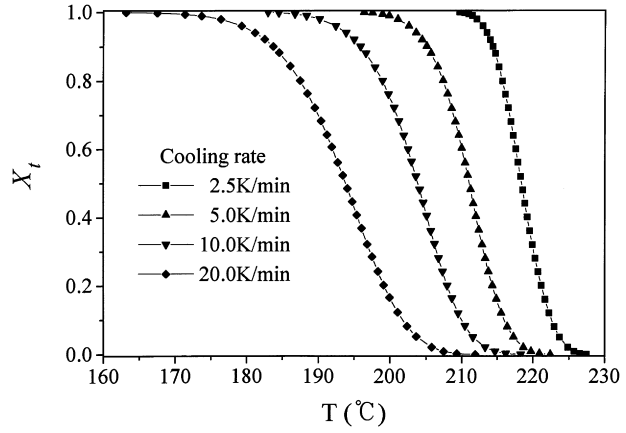

Fig. 7. Plots of relative crystallinity X_t versus crystallization temperature for PET homopolymer crystallized non-isothermally at various cooling rates.

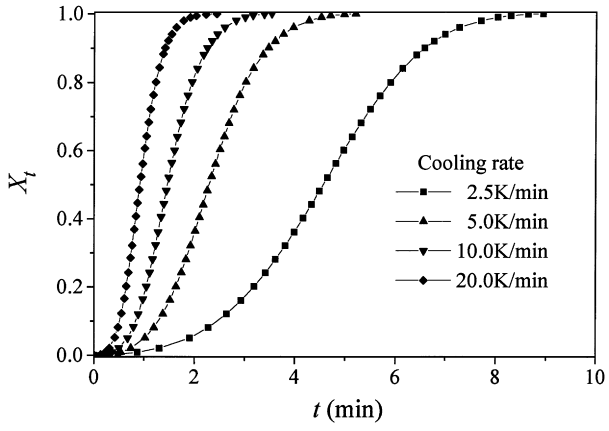

Fig. 8. Plots of relative crystallinity X_t versus crystallization time for PET hompolymer crystallized non-isothermally at various cooling rates.

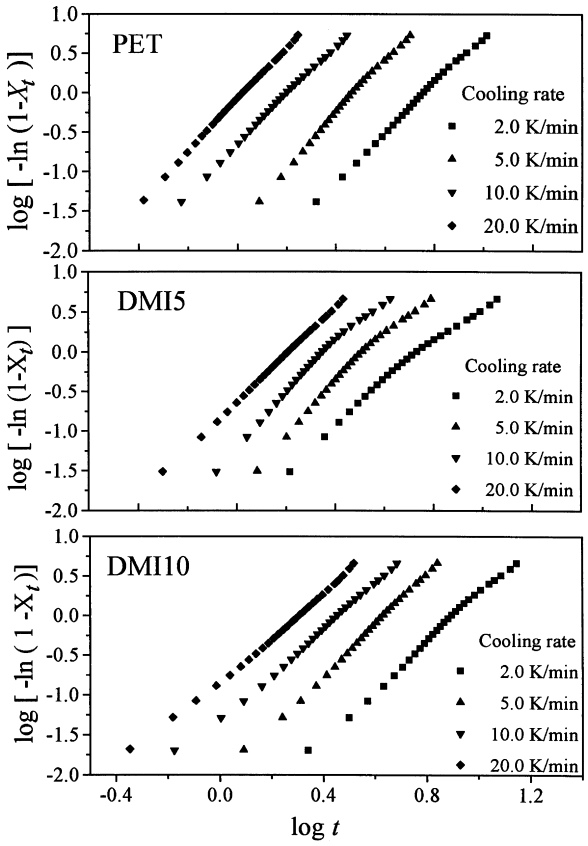

Fig. 9. Avrami plots of relative crystallinity X_t for PET homopolymer and PEIT copolyesters crystallized with various cooling rates: DMI5, PEIT (5.0 mol% DMI) copolyester; DMI10 (10.0 mol% DMI) copolyester.

spherulite impingement occurred in the later stage of crystallization. Commonly, the secondary crystallization stage is regarded as the perfection of crystal. In contrast, the first regime behaviors measured might result from the nucleation and growth, so-called primary crystallization, occurred in the early stage. In general, the modified Avrami analysis is valid only for the first regime, i.e. the crystallization at the early stage. Thus, for each cooling run the Avrami parameters were estimated from the slope and intercept of the plot of $\log[-\ln(1 - X_t)]$ versus $\log t$ for the primary crystallization which takes place in the early stage. The results are summarized in Table 4.

Table 4
Avrami parameters of PET homopolymer and PEIT copolyesters

Polyester	Avrami parameters[a]	Cooling rate (K/min)			
		2.0	5.0	10.0	20.0
PET	n	2.8	3.2	3.3	3.4
	k'	0.0946	0.5462	0.8613	0.9921
	$t_{1/2}$	2.03	1.08	0.94	0.89
DMI5	n	2.9	3.4	3.5	3.1
	k'	0.0821	0.5060	0.8300	0.9491
	$t_{1/2}$	2.08	1.10	0.95	0.90
DMI10	n	3.4	3.4	3.1	2.8
	k'	0.0320	0.3738	0.7268	0.9054
	$t_{1/2}$	2.51	1.20	0.98	0.91

[a] n is the Avrami exponent, k' the corrected rate constant of crystallization, and $t_{1/2}$ the crystallization half-time.

For the primary crystallization of PET homopolymer, Avrami exponent n was estimated to be 2.81–3.37, depending upon the cooling rates. Here, it is useful to compare the values of the Avrami exponent determined in this study with those reported previously in the literature. Phillips and Manson [13] measured $n = 3.1$ for the non-isothermal crystallization under a cooling rate of 3.0–10.0 K/min, so that they concluded that PET homopolymer crystallizes through three-dimensional spherulitic growth with a predominant heterogeneous nucleation. In contrast, Jeziorny [33] reported $n = 2.35$–2.65 for cooling runs with a rate of 8.5–17.0 K/min. With these results he suggested that there is the existence of three-dimensional spherulites which form as a result of heterogeneous nucleation. In comparison, the values of the Avrami exponent in our study are comparable with that of Phillips and Manson, but slightly higher than those of Jezorny. In conclusion, the values of the Avrami exponent in our study suggest that for the PET hompolymer the non-isothermal crystallization in the early stage follows either three-dimensional growth with heterogeneous nucleation or two-dimensional growth with homogeneous nucleation. However, the PET homopolymer sample might contain some residues of the catalysts which were used in the polymerization. The residues of the catalysts may play a role as nuclei. Therefore, the non-isothermal crystallization in the PET homopolymer studied here might follow a heterogeneous nucleation and three-dimensional spherulitic growth.

The non-isothermal crystallization exotherms of DMI5 and DMI10 copolyesters in Fig. 6 were analyzed in the same manner as those of the PET homopolymer. Their plots of $\log[-\ln(1 - X_t)]$ versus $\log t$ are illustrated in Fig. 9. On the modified Avrami plot, these copolyesters also reveal two-regime behaviors similar to those observed for the PET homopolymer. For the primary crystallization of the copolyesters, Avrami exponents n have been estimated and compared with those of the PET homopolymer in Table 4. It is turned out that similar values of the Avrami exponent were obtained for the DMI5 and DMI10 copolyesters. Therefore, it is also suggested that the non-isothermal crystallizations of the PEIT copolyesters follow a heterogeneous nucleation and three-dimensional spherulitic growth as occurring in the PET homopolymer. In conclusion, the type of nucleation and spherulitic growth in the PET polymer is not influenced by incorporating DMI unit into the polymer backbone.

However, the crystallization rate is dependent upon the cooling rate. For the PET homopolymer, the crystallization rate constant (k') increases with increasing cooling rate, whereas the crystallization half-time ($t_{1/2}$) decreases with increasing cooling rate (see Table 4). Similar trends in both the k' and $t_{1/2}$ are observed for the DMI5 and

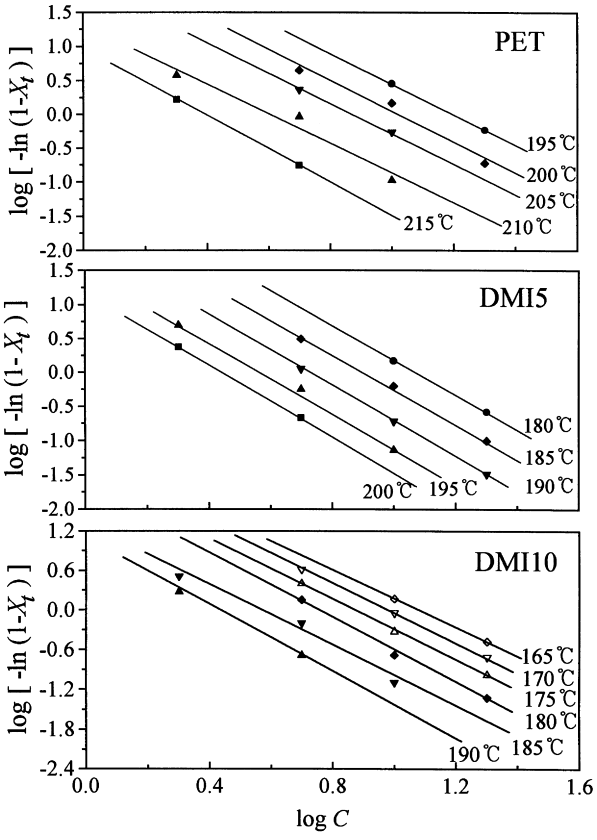

Fig. 10. Ozawa plots of relative crystallinity X_t for PET homopolymer and PEIT copolyesters crystallized with various cooling rates: DMI5, PEIT (5.0 mol% DMI) copolyester; DMI10 (10.0 mol% DMI) copolyester. The filled symbols were measured by DSC and the solid lines were fitted by Eq. (12).

DMI10 copolyesters. However, both the k' and $t_{1/2}$ are influenced by the DMI content in the copolyester: that is, the k' at a chosen cooling rate became small and the $t_{1/2}$ large as the content of DMI unit increased. Conclusively, the crystallization rate is accelerated by increasing the cooling rate, but retarded by incorporating the DMI unit into the polymer backbone.

3.3.2. Ozawa analysis

Ozawa [19,20] has extended the Avrami theory for isothermal crystallization to the non-isothermal case by assuming that the sample is cooled with a constant rate from the molten state. In the Ozawa approach, the time variable in the Avrami equation is replaced by a cooling rate. Thus, the relative crystallinity X_t is described as a function of constant cooling rate C as:

$$X_t = 1 - \exp\left(\frac{-K(T)}{C^m}\right) \tag{11}$$

where $K(T)$ is the cooling function at temperature T and m is the Ozawa exponent. Here, the Ozawa exponent is similar to the Avrami exponent, which depends on the type of nucleation and growth mechanism. Double logarithms of Eq. (11) and rearrangement result in the following form:

$$\log[-\ln(1 - X_t)] = \log K(T) - m \log C. \tag{12}$$

The non-isothermal crystallization exotherms of the PET and its copolyesters in Fig. 6 were analyzed using Eq. (12). The results are illustrated in Fig. 10. For the non-isothermal crystallizations of PET homopolymer, plots of $\log[-\ln(1 - X_t)]$ versus $\log C$ are reasonably linear as reported previously in the literature [19,35]. Thus, the Ozawa exponent (m)s and the cooling function ($K(T)$)s have been determined from the slope and intercept of the plots, and summarized in Table 5. The exponent m and the logarithmic cooling function $\log K(T)$ are 2.1–2.5 and 0.958–2.726, respectively, depending upon the temperature over 195–215℃.

Here, the values of the exponent m in this study are worth comparing with the results reported previously. Ozawa [19] reported $m = 3.4$–3.6 for PET polymer crystallized with a cooling rate of 1.0–4.0 K/min. Ozawa suggested that the non-isothermal crystallization in PET homopolymer follows a homogeneous nucleation and three-dimensional spherulitic growth. However, Jabarin [35] obtained $m = 2.5$–2.8 for the non-isothermal crystallization with a cooling rate of 5.0–20.0 K/min, concluding that a heterogeneous nucleation and three-dimensional spherulitic growth occur in the non-isothermal crystallization of PET polymer. In

Table 5
Ozawa exponents and cooling functions of PET hompolymer and PEIT copolyesters

Temperature (℃)	PET homopolymer		DMI5 copolyester		DMI10 copolyester	
	m	$\log K(T)$	m	$\log K(T)$	m	$\log K(T)$
215	2.5	0.958	—	—	—	—
210	2.2	1.311	—	—	—	—
205	2.1	1.821	—	—	—	—
200	2.3	2.309	2.6	1.166	—	—
195	2.3	2.726	2.5	1.484	—	—
190	—	—	2.6	1.836	2.4	1.002
185	—	—	2.5	2.256	2.3	1.248
180	—	—	2.5	2.669	2.5	1.830
175	—	—	—	—	2.3	1.989
170	—	—	—	—	2.2	2.149
165	—	—	—	—	2.1	2.306

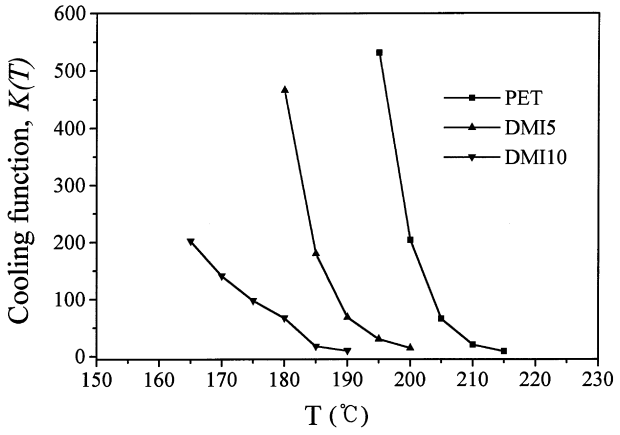

Fig. 11. Variations of cooling function versus crystallization temperature for PET hompolymer and PEIT copolyesters crystallized with various cooling rates: DMI5, PEIT (5.0 mol% DMI) copolyester; DMI10 (10.0 mol% DMI) copolyester.

comparison, the values of the exponent m in the present study are much lower than those reported by Ozawa and, however, very close to those obtained by Jabarin. And, at 190–195°C the values of $\log K(T)$ are in good agreement with those reported by Jabarin. Therefore, the statement of Jabarin may be applicable for the non-isothermal crystallization of PET polymer in this study.

In addition, it is noted that the values of the Ozawa exponent m are relatively smaller than those (2.8–3.4) of the Avrami exponent n which were obtained by the modified Avrami analysis in the earlier section. That is, the Ozawa exponent is always smaller than the Avrami exponent by 0.7–0.9. A similar situation has been reported for the non-isothermal crystallizations of other polymers, such as poly(ether ether ketone) [17], poly(aryl ether ether ketone ketone) [36], and poly(hydroxy ether of bisphenol-A)/poly(ϵ-caprolactone) blend [18]. These results are evident that there is a big discrepancy between both of the analyses even though they have been derived from the same Avrami approach.

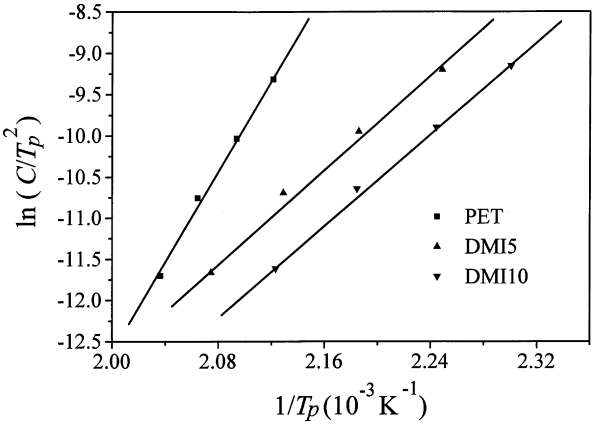

Fig. 12. Kissinger plots of PET homopolymer and PEIT copolyesters crystallized with various cooling rates: DMI5, PEIT (5.0 mol% DMI) copolyester; DMI10 (10.0 mol% DMI) copolyester. The filled symbols were measured by DSC and the solid lines were fitted by Eq. (13).

The Ozawa exponent and cooling function were estimated for the DMI5 and DMI10 copolyesters. For the DMI5 copolyester, the exponent m and cooling function $\log K(T)$ are 2.5–2.6 and 1.166–2.669 over 180–200°C, respectively. For the DMI10 copolyester, the exponent m and cooling function $\log K(T)$ are 2.1–2.5 and 1.002–2.306 over 165–190°C, respectively. In comparison, the exponents m and cooling functions $\log K(T)$ of the PEIT copolyesters are very close to those of the PET homopolymer, respectively. This suggests that the non-isothermal crystallization of PEIT copolyester follows the same nucleation and growth mechanism of PET homopolymer.

The cooling function $K(T)$ is a function of nucleation and growth rate [19,20]. For the PET homopolymer, the $K(T)$ increases exponentially with decreasing temperature (see Fig. 11). In fact, the thermodynamic driving force for crystallization increases as the crystallization temperature lowers until the temperature which causes a big increment in the viscosity so that the transport of polymer chains to the growth point becomes very difficult. Therefore, the result observed in the PET polymer is natural.

Similar dependencies of $K(T)$ to the crystallization temperature were detected for the DMI5 and DMI10 copolyesters. In comparison, while decreasing the crystallization temperature the $K(T)$ in the copolyester however increases more slowly than in the PET homopolymer. This trend is pronounced further as the content of DMI unit in the copolyester increases. This might result from the chain irregularity due to the *meta*-linked DMI unit on the polymer backbone which hinders the polymer chains to pack each other in a regular manner. That is, the PEIT copolyesters containing the irregular DMI units take relatively longer time in the crystallization than does the PET homopolymer.

3.4. Activation energy of non-isothermal crystallization

In a non-isothermal crystallization, the activation energy E_a can be derived from the variation of crystallization peak temperature T_p with cooling rate by the Kissinger approach [37] as follows:

$$\frac{\mathrm{d}(\ln(C/T_p^2))}{\mathrm{d}(1/T_p)} = -\frac{E_a}{R} \tag{13}$$

where R is the universal gas constant. The Kissinger plotting was performed for the T_ps and cooling rates (C)s in Table 3 which were measured for the PET and its copolyesters (see Fig. 12). Overall, for all the polymers the Kissinger plots exhibit a relatively good linearity. The crystallization activation energy was estimated from the slope in the plot.

The E_a is estimated to be −230.0 kJ/mol for the PET homopolymer, −116.3 kJ/mol for the DMI5 copolyester and −114.4 kJ/mol for the DMI10 copolyester. Here, the crystallization is exothermic, so that the activation energy is negative. In comparison, the E_a of the PET polymer is almost two times lower than those of the DMI5 and DMI10

copolyesters. And, the E_a of the DMI5 copolyester is slightly lower than that of the DMI10 copolyester.

In the view of kinetics, the activation energy can be correlated to the crystallization rate. As described earlier in this study, the crystallization rate constant k', which was estimated by the modified Avrami analysis, decreases relatively in the order PET > DMI5 > DMI10 (see Table 4). The cooling function $K(T)$ obtained by the Ozawa analysis is also in the decreasing order PET > DMI5 > DMI10. That is, the lower activation energy of crystallization drives the more rapid crystallization rate. These may result from fact that the more regular PET polymer chains are packed more easily in an ordered manner than do the less regular PEIT copolyester chains.

4. Conclusions

PET, PEI and their copolyesters with reasonably high molecular weights were synthesized with varying composition from DMT, DMI and EG monomers via a conventional bulk polycondensation reaction. Their chemical compositions and molecular weights were characterized by ^{1}H NMR spectroscopy and capillary viscometry, respectively. Thermal behaviors of the copolyesters were investigated by DSC: both T_g and T_m of the copolyester were affected severely by its composition.

Non-isothermal crystallization thermograms of PET and its copolyesters containing DMI unit of $\leq$10 mol% were measured by DSC and their crystallization kinetics were investigated fairly by both modified Avrami and Ozawa analyses. Regardless of the PET homopolymer or its copolyesters, the value of the Avrami exponent is 2.8–3.5, depending on the cooling rate, whereas the value of the Ozawa exponent is 2.1–2.6, depending on the temperature. These results inform us two things: First, in the non-isothermal crystallization under a constant cooling rate the nucleation and growth mechanism of the PEIT copolyester is same as that of the PET homopolymer. That is, the nucleation and growth mechanism of the PET homopolymer is not affected by incorporating the non-crystallizable or poorly crystallizable DMI units into the polymer backbone. Second, the values of the Avrami exponent are always higher than those of the Ozawa exponent by 0.7–0.9. This indicates a big discrepancy between both of the analyses even though they have been derived from the same Avrami approach.

However, the crystallization rate of the PET homopolymer is influenced by the composition as well as the cooling rate. The crystallization rate is decreased by incorporating the DMI unit into the polymer backbone and also by lowering the cooling rate. A similar effect of the cooling rate on the crystallization is observed for the PEIT copolyesters.

In addition, for the PET homopolymer and its copolyesters the activation energies of non-isothermal crystallization were estimated by the Kissinger approach. The crystallization activation energy is affected by the composition which is the primary factor to influence the crystallization rate: that is, the crystallization activation energy is increased by incorporating the DMI unit into the polymer backbone.

Acknowledgements

This study was supported in part by Pohang Irons and Steel Company (POSCO) and by the Ministry of Education via the School of Environmental Engineering, POSTECH (3ER9811101) and the Basic Research Institute Program (BSRI-97-3438).

References

[1] Brozenic NJ. Modern plastics encyclopedia. New York: McGraw-Hill, 1986.
[2] Chemical and Engineering News, April 18, 1994.
[3] Goodman I. In: Mark HF, Gaylord NG, Bikales NM, editors. Encyclopedia of polymer science and technology, 11. New York: Wiley, 1969. p. 1.
[4] Yamadera R, Murano M. J Polym Sci Part A-1 1967;5:2259.
[5] Hsiue G-H, Yeh T-S, Chang S. J Appl Polym Sci 1989;37:2803.
[6] Kanda K, Okamura T, Minamiki T, Inoue T, Kondoo Y. Korean Patent, No. 85-1958.
[7] Ooniwa N, Kato H, Kondo T. Korean Patent, No. 93-19864.
[8] Matsui K, Natakawa Y, Tanaka A, Inoue T. Korean Patent, No. 92-9046.
[9] Heyes PJ, White CH, Singh H, European Patent, No. 384 606.
[10] Greener J, Gillmor JR, Daly RC. Macromolecules 1993;26:6416.
[11] Pasquarelli O. SPE Seventh Int. Conf. High Performance Plastics Containers, 1986.
[12] Wallach ML. Makromol Chem 1967;19:103.
[13] Phillips R, Manson JAE. J Polym Sci Part B: Polym Phys 1997;35:875.
[14] Baker CH, Mandelkern L. Polymer 1966;7:7.
[15] Dimarzio EA, Gibbs JH. J Polym Sci 1959;40:121.
[16] Herrero CH, Acosta JL. Polymer J 1994;26:786.
[17] Cebe P. Polym Composites 1988;9:271.
[18] de Juana R, Jauregui A, Calahorra E, Cortazar M. Polymer 1996;37:3339.
[19] Ozawa T. Polymer 1971;12:150.
[20] Ozawa T. Polymer 1978;19:1142.
[21] Ziabicki A. Appl Polym Symp 1967;6:1.
[22] Ziabicki A. Coll Polym Sci 1974;6:252.
[23] Caze C, Devaux E, Crespy A, Cavrot JP. Polymer 1997;38:497.
[24] Choe CR, Lee KH. Polym Engng Sci 1988;29:801.
[25] Caze C, Devaux E, Crespy A, Cavrot JP. Polymer 1997;38:497.
[26] Douillard A, Dumazet Ph, Chabert B, Guillet J. Polymer 1993;34:1702.
[27] Chan TW, Isayev AI. Polym Engng Sci 1994;34:461.
[28] Nakamura K, Katayama K, Amano T. J Appl Polym Sci 1973;17:1031.
[29] Kamal MR, Chu E. Polym Engng Sci 1983;23:27.
[30] Patel RM, Spruiell JE. Polym Engng Sci 1991;31:730.
[31] Avrami M. J Chem Phys 1939;7:1103.
[32] Avrami M. J Chem Phys 1940;8:212.
[33] Wunderlich B. Macromolecular physics. New York: Academic Press, 1976.
[34] Jeziorny A. Polymer 1978;19:1142.
[35] Jabarin SA. J Appl Polym Sci 1987;34:97.
[36] Liu T, Mo Z, Wang S, Zhang H. Polym Engng Sci 1997;37:568.
[37] Kissinger HE. J Res Natl Stds 1956;57:217.